

Energetic and Structural Interactions between δ -Dendrotoxin and a Voltage-gated Potassium Channel

John P. Imredy and Roderick MacKinnon*

Howard Hughes Medical
Institute, Laboratory of
Molecular Neurobiology and
Biophysics, Rockefeller
University, New York
NY 10021, USA

Dendrotoxin proteins isolated from Mamba snake venom block potassium channels with a high degree of specificity and selectivity. Using site-directed mutagenesis we have identified residues that constitute the functional interaction surfaces of δ -dendrotoxin and its voltage-gated potassium channel receptor. δ -Dendrotoxin uses a triangular patch formed by seven side-chains (Lys3, Tyr4, Lys6, Leu7, Pro8, Arg10, Lys26) to block K^+ currents carried by a Shaker potassium channel variant. The inhibitory surface of the toxin interacts with channel residues at Shaker positions 423, 425, 427, 431, and 449 near the pore. Amino acid mutations that interact across the toxin-channel interface were identified by mutant cycle analysis. These results constrain the possible orientation of dendrotoxin with respect to the K^+ channel structure. We propose that dendrotoxin binds near the pore entryway but does not act as a physical plug.

© 2000 Academic Press

*Corresponding author

Keywords: *Dendroaspis angusticeps*; snake dendrotoxin; Shaker; Kv1.1; KcsA

Introduction

Here we study the energetic interaction between two proteins, a voltage-dependent K^+ channel and a specific inhibitor from snake venom, δ -dendrotoxin. Our aim is to understand the mechanism by which δ -dendrotoxin inhibits ion flow, and by so doing, gain deeper insight into the operation of the channel.

A single dendrotoxin molecule associates reversibly with the K^+ channel to produce the inhibited state. The electrophysiological assay used in this study provides an accurate determination of the equilibrium constant for the binding reaction between the toxin and channel proteins. Scanning mutagenesis was applied to both proteins to identify the amino acids involved in toxin-channel complexation, and thermodynamic mutant cycle analysis to correlate pairs of amino acids that are coupled energetically across the protein-protein interface. When the known structures of the KcsA K^+ channel and dendrotoxin homologues are considered, the energetic data reveal well-defined interaction surfaces on both the K^+ channel and

the dendrotoxin and suggest a somewhat unconventional mechanism of inhibition.

With what degree of confidence can mutant cycle data be used to deduce structural information in a protein-protein complex? Two studies addressed this question. First, Schreiber & Fersht (1995) compared the magnitude of mutant cycle coupling energies with distances measured in the crystallographic structure of the enzyme barnase in complex with its inhibitor barstar. The strength of coupling between mutations at two sites was strongly correlated with distance. Most coupling energies greater than $1.0 \text{ kcal mol}^{-1}$ involved amino acids that were within 4 \AA of each other. Second, work from our own laboratory attempted to deduce the surface structure of the scorpion toxin binding site on K^+ channels (Hidalgo & MacKinnon, 1995). The scorpion toxin structure, serving as a distance caliper to interpret mutant cycle data, provided a model of the surface that included the positions of several key channel amino acids (Ranganathan *et al.*, 1996). The subsequent structure determination of the KcsA K^+ channel by X-ray crystallography confirmed that the predictions based on the mutant cycle analysis were surprisingly good (Doyle *et al.*, 1998; MacKinnon *et al.*, 1998). Thus, it seems reasonable to expect that energetic interactions on the surfaces of rigid, interacting proteins should be fairly additive, and therefore useful structural

Present address: J. P. Imredy, Department of Pharmacology, Merck Research Laboratories, WP46-300, West Point, PA 19486, USA.

E-mail address of the corresponding author: mackinn@rockvax.rockefeller.edu

spondingly fast, but such experiments are costly in terms of the quantity of toxin required. Thus, the ShaKv1.1 channel, with a K_d for δ -dendrotoxin in the nanomolar range, was used as the "wild-type" channel in this study.

The K⁺ current carried by ShaKv1.1 channels expressed in frog oocytes was measured by repeated application of short membrane-depolarizing voltage pulses in order to open the voltage-dependent channels (Figure 1(b) and (c)). Dendrotoxin was applied by bath perfusion while monitoring K⁺ current (Figure 1(b)). Extracellular application of a high concentration of dendrotoxin was used in order to determine the background current (dendrotoxin insensitive current) which was subtracted from the total measured current prior to analysis. The fraction of uninhibited K⁺ current as a function of the δ -dendrotoxin concentration is shown (Figure 1(d)). The data, which adhere to a Langmuir isotherm with 1:1 stoichiometry between toxin and channel ($K_d = 2.0$ nM), emphasize the precision with which the K_d can be determined for the reversible inhibition reaction.

At extremely high concentrations, dendrotoxin inhibits the K⁺ channels in an irreversible manner, as shown (Figure 1(b)). We do not yet understand this irreversible inhibition, but it is distinct and separable from the reversible process that is the focus of the present study.

The functional interaction surface of δ -dendrotoxin

The known structure of dendrotoxin-K, with 55 out of 57 residues identical with δ -dendrotoxin, was used to guide our mutagenesis of surface amino acids (Berndt *et al.*, 1993). We mutated 28 out of 57 amino acid residues on δ -dendrotoxin, including all ionizable and solvent-exposed side-chains. Each mutant toxin was expressed in *Escherichia coli*, purified by sequential ion exchange and reversed-phase chromatography, and stored for electrophysiological assay. Figure 2(a) shows the amino acid sequence of δ -dendrotoxin and the positions of the mutated residues. All mutations were to an Ala residue, except where this amino acid occurred in the wild-type sequence, in which case the substitution was to a Gln residue.

Figure 2(b) graphs the change in binding free energy resulting from each mutation. The binding free energy was derived from the inhibition constant measured as in Figure 1(d) for each dendrotoxin mutant (see Table 1). A total of five out of the seven mutants with the largest changes (>1.5 kcal mol⁻¹) fall within the first ten positions of the N-terminal region of δ -dendrotoxin (Lys3, Tyr4, Lys6, Pro8 and Arg10). Interestingly, this region is least conserved among members of the dendrotoxin family (Dufton, 1985; Gasparini *et al.*, 1998; Harvey, 1997). Additional functionally significant mutations include Lys26Ala and Arg44Ala. Figure 2(c) presents these results in color displayed over the accessible surface of each mutated amino

acid. The color scale correlates increased changes in the binding free energy with an increased red-shift, starting with blue for no change and ending with red for the largest alteration of binding free energy (3.5 kcal mol⁻¹).

All but one functionally significant residue (Arg44) fall within a triangular patch (~ 20 Å each side) on the wider end of the pear-shaped toxin (Figure 2(c), top). The vertices of this triangle are demarcated by amino acids Lys3, Arg10 and Lys26. The outlying residue, Arg44, has its side-chain buried in the structure of dendrotoxin-K. It is therefore possible that mutation of Arg44 has induced a global conformational change of the toxin (Beeser *et al.*, 1997; Gasparini *et al.*, 1998). Our results are in very good agreement with those reported by Menez and colleagues (Gasparini *et al.*, 1998) who, using a biochemical binding assay, defined a similarly located patch of functionally important residues for the interaction of α -dendrotoxin with rat brain synaptosomes.

The triangular interaction surface on δ -dendrotoxin includes amino acid residues Lys3, Tyr4, Lys6, Leu7, Pro8, Arg10 and Lys26. The mutation Leu7Ala was "silent", but when defining an interaction surface on the basis of function, a null hypothesis must be applied. That is, a mutation probably involves an interaction surface amino acid in order to perturb the binding energy (assuming there are no long-range conformational changes), but the absence of perturbation does not exclude a residue's presence on the surface. The "hot spots" of binding energy on the interface of growth hormone and its receptor provided a very nice demonstration of this fact (Clackson & Wells, 1995). Because Leu7 is located at the center of the functionally defined triangle, we assume that it interfaces with the K⁺ channel, even though its mutation to Ala was without effect.

The functional interaction surface incorporates residues from various structural elements of the toxin (Figure 2(a)). Figure 2(c) shows a ribbon diagram of these elements. Residues 3, 4, 6 and 7 are part of the amino-terminal 3_{10} helix, while residues 8 and 10 emerge from the loop connecting the 3_{10} helix with the narrow tip of the toxin. Lys26 juts out from a hairpin turn between the two beta strands forming the back side of this view of the toxin. The highly positively charged interaction surface (containing three lysine residues and one arginine residue) argues for the probable indispensable role of basic residues in the binding of toxins targeting the pore region of cation-selective channels (Becker *et al.*, 1992; Park & Miller, 1992a). Interestingly, there is no overlap between the active site of the structurally similar protease inhibitors (which corresponds to residues 15-17 of δ -dendrotoxin) and the active site of dendrotoxins (Gasparini *et al.*, 1998; Smith *et al.*, 1997; Wang *et al.*, 1999).

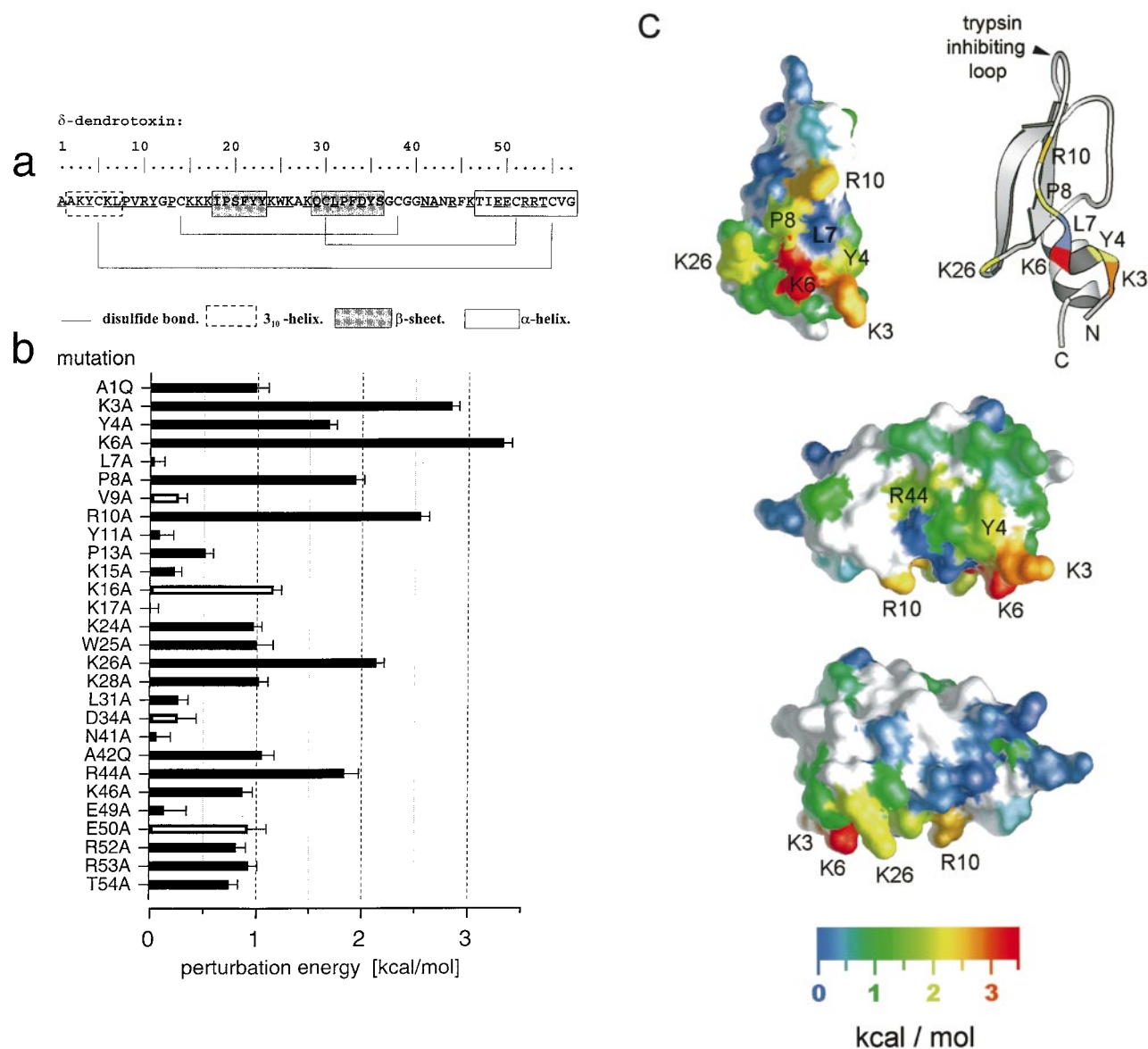


Figure 2. Interaction surface of δ -dendrotoxin. (a) Sequence of δ -dendrotoxin. Underlined residues indicate the point substitutions by alanine (or glutamine for wild-type alanine), each of which was synthesized in *E. coli*, purified, and tested against ShaKv1.1. The secondary structural elements, as well as the cystine bonds are diagrammed. (b) Bar graph showing the change in binding energy relative to wild-type δ -dendrotoxin arising from the indicated point mutation. The absolute value of the change in binding energy (kcal mol^{-1}) was calculated according to: $|0.6 \ln\{K_d \text{ mut}/K_d \text{ wt}\}|$. Filled and empty bars denote a decrease or increase in toxin affinity, respectively. Table 1 (column 2) lists the K_d values obtained as in Figure 1(b)-(d) for each point mutant. The error bar represents the calculated error arising from propagation of the measured error in each K_d value (see Materials and Methods). (c) Surface representations of δ -dendrotoxin viewed from three orientations. The structure of dendrotoxin-K (Berndt *et al.*, 1993; Acc. No.: 1DTK), which is 96% identical with δ -dendrotoxin, was used as a structural model for δ -dendrotoxin. The surface color indicates the change in binding energy resulting from mutation of the underlying residue according to the color scale below. Non-mutated surface regions are white. Labeled residues are those with binding energy changes $>1.5 \text{ kcal mol}^{-1}$. Top left-hand panel, Orientation of the toxin showing the functional interaction surface of dendrotoxin. Leu7 was included as part of the interaction surface (see the text). Top right-hand panel, Ribbon representation of δ -dendrotoxin using identical view as in the left-hand panel. Middle and bottom, Opposing side views of the dendrotoxin binding surface. The molecular surface representations for this and all subsequent Figures were calculated and drawn using GRASP (Nicholls *et al.*, 1991). The ribbon representation was drawn with MOLSCRIPT (Kraulis, 1991).

Table 1. Dissociation constants and coupling energies of δ -dendrotoxin and ShaKv1.1 K⁺ channel mutations

SkaKv1.1	Wild-type			L425-N427S			E4233A		D431A		Y449	
δ -DTX	K_d (nM) \pm SEM(<i>n</i>)	K_d (pM) \pm SEM(<i>n</i>)	Coupling (kcal/mol) \pm SEM	K_d (nM) \pm SEM(<i>n</i>)	Coupling (kcal/mol) \pm SEM	K_d (nM) \pm SEM(<i>n</i>)	Coupling (kcal/mol) \pm SEM	K_d (nM) \pm SEM(<i>n</i>)	Coupling (kcal/mol) \pm SEM			
wild-type	2 \pm 0.2 (5)	2.2 \pm 0.8 (6)		15.5 \pm 4.5 (4)		316 \pm 27 (8)		214 \pm 9 (5)				
A1Q	10.4 \pm 2 (5)	12.2 \pm 2.8 (6)	0.04 \pm 0.41									
K3A	230 \pm 17 (5)	675 \pm 245 (6)	0.59 \pm 0.43	1010 \pm 123 (5)	0.34 \pm 0.3	614 \pm 26 (6)	2.44 \pm 0.15	1244 \pm 230 (5)	1.79 \pm 0.21			
Y4A	33.4 \pm 2.5 (5)	55 \pm 2.6 (4)	0.24 \pm 0.33	321 \pm 29 (4)	0.13 \pm 0.29	1918 \pm 202 (5)	0.61 \pm 0.17	422 \pm 73 (5)	1.28 \pm 0.2			
K6A	518 \pm 55 (5)	610 \pm 90 (7)	0.04 \pm 0.36	1952 \pm 120 (4)	0.43 \pm 0.29	4630 \pm 460 (6)	1.72 \pm 0.18	5280 \pm 631 (5)	1.41 \pm 0.18			
L7A	2.1 \pm 0.3 (5)	28.9 \pm 2.3 (5)	1.51 \pm 0.35	132 \pm 15 (5)	1.25 \pm 0.32	408 \pm 35 (4)	0.12 \pm 0.2	223 \pm 25 (6)	0 \pm 0.2			
P8A	51 \pm 5 (4)	55.6 \pm 13 (7)	0.01 \pm 0.38	472 \pm 100 (4)	0.11 \pm 0.33	1874 \pm 97 (6)	0.87 \pm 0.16	330 \pm 42 (5)	1.68 \pm 0.18			
V9A	1.3 \pm 0.1 (4)	5.3 \pm 0.7 (6)	0.27 \pm 0.35									
R10A	142 \pm 14 (5)	48.6 \pm 8.2 (5)	0.7 \pm 0.36	291 \pm 23 (5)	0.8 \pm 0.29	2900 \pm 330 (6)	1.23 \pm 0.19	2953 \pm 785 (4)	0.98 \pm 0.27			
Y11A	2.3 \pm 0.5 (4)	2.5 \pm 0.3 (4)	0.01 \pm 0.39									
P13A	4.7 \pm 0.4 (4)	9.4 \pm 2.2 (5)	0.36 \pm 0.38									
K15A	2.9 \pm 0.2 (4)	5.6 \pm 0.8 (4)	0.34 \pm 0.35									
K16A	0.29 \pm 0.02 (4)	0.84 \pm 0.11 (4)	0.58 \pm 0.51									
K17A	2 \pm 0.16 (4)	2.5 \pm 0.36 (4)	0.08 \pm 0.35									
K24A	10.1 \pm 0.9 (5)	9.5 \pm 1 (4)	0.09 \pm 0.34									
W25A	10.6 \pm 3 (4)	30.6 \pm 5 (4)	0.58 \pm 0.43									
K26A	71 \pm 6 (5)	81.7 \pm 13 (5)	0.03 \pm 0.36	265 \pm 29 (6)	0.44 \pm 0.3	2600 \pm 110 (6)	0.88 \pm 0.15	1851 \pm 275 (5)	0.85 \pm 0.19			
K28A	11 \pm 1.3 (5)	7 \pm 2 (4)	0.33 \pm 0.41									
L31A	3.1 \pm 0.4 (4)	3.5 \pm 0.6 (4)	0.02 \pm 0.37									
D34A	1.3 \pm 0.3 (4)	2.1 \pm 0.9 (5)	0.23 \pm 0.88									
N41A	2.2 \pm 0.5 (4)	8.1 \pm 1 (4)	0.72 \pm 0.39									
A42Q	11.6 \pm 2.2 (4)	35.8 \pm 5.6 (5)	0.62 \pm 0.39									
R44A	43 \pm 10 (4)	55.6 \pm 17 (6)	0.1 \pm 0.45									
K46A	8.5 \pm 1.2 (4)	3.9 \pm 0.5 (4)	0.52 \pm 0.36									
E49A	2.5 \pm 1 (4)	2 \pm 0.5 (5)	0.08 \pm 0.68									
E50A	0.43 \pm 0.1 (4)	0.99 \pm 0.18 (7)	0.44 \pm 0.6									
R52A	7.7 \pm 1 (5)	10.8 \pm 1.3 (5)	0.15 \pm 0.36									
R53A	9.4 \pm 1 (4)	5.5 \pm 0.67 (4)	0.38 \pm 0.35									
T54A	6.9 \pm 0.8 (4)	2.9 \pm 0.45 (4)	0.58 \pm 0.36									

ShaKv1.1	δ -DTX, K_d (nM)
Y415A	2.9 \pm 0.4 (4)
F416A	2.8 \pm 1 (4)
E418A	No expression
E420A	7.5 \pm 2.1 (4)
E421A	4.2 \pm 1.6 (4)
L425A	7.6 \pm 1.2 (4)
F426A	4.4 \pm 1 (4)
N427A	2.2 \pm 0.7 (4)
V451A	6.2 \pm 2 (4)
G452A	0.4 \pm 0.1 (7)
V453A	2.3 \pm 0.45 (5)
W454A	1.7 \pm 0.2 (4)

The affinities for ShaKv1.1 of δ -dendrotoxin variants are listed in the second column from the left (wild-type). Across the top row are listed those ShaKv1.1 mutations which resulted in significant changes in the dissociation constant when screened against wild-type δ -dendrotoxin. Note that the affinities for the ShaKv1.1 double mutant Leu425His/Asn427Ser are listed in units of picomolar. The boxed inset at lower right contains the equilibrium dissociation constants corresponding to those channel mutations whose effects on δ -dendrotoxin binding were small. The intersections between rows and columns present both the dissociation constant, K_d , for the combination of toxin and channel mutant as well as the coupling energy between those two mutations calculated according to equation (1). In parentheses are the number of oocyte recording trials used to obtain the dissociation constant. The coupling energies >1 kcal mol⁻¹ are plotted in Figure 4(a) and color mapped onto the surface of the K⁺ channel KcsA (Figure 4(b)).

The dendrotoxin receptor surface on the potassium channel

The conserved sequence of the pore region of K⁺ channels forms the selectivity filter that catalyzes the rapid diffusion of K⁺ across the membrane barrier to the virtual exclusion of all other cations. Based on the KcsA K⁺ channel structure, we know that four identical pore regions come together to form the filter. Each monomer contains a loop, termed the "turret", that juts out into the extracellular solution as if to guard the centrally located pore entryway. To identify amino acids of the ShaKv1.1 channel that interact with δ -dendrotoxin,

we produced mutations at sites known to be at the surface of the closely related KcsA K⁺ channel (Doyle *et al.*, 1998). Figure 3(a) indicates the mutations made in this study. A total of 15 amino acids along the pore region were substituted, one at a time, by an alanine residue. In addition, a double substitution was made which conferred Kv1.1 turret sequence identity onto ShaKv1.1 (see Figure 1(a)).

Figure 3(b) graphs the changes in binding free energy resulting from the mutations (from Table 1), while Figure 3(c) displays the same data in color on the surface of the KcsA K⁺ channel. Mutation of amino acids at positions 423, 425/427, 431 and 449

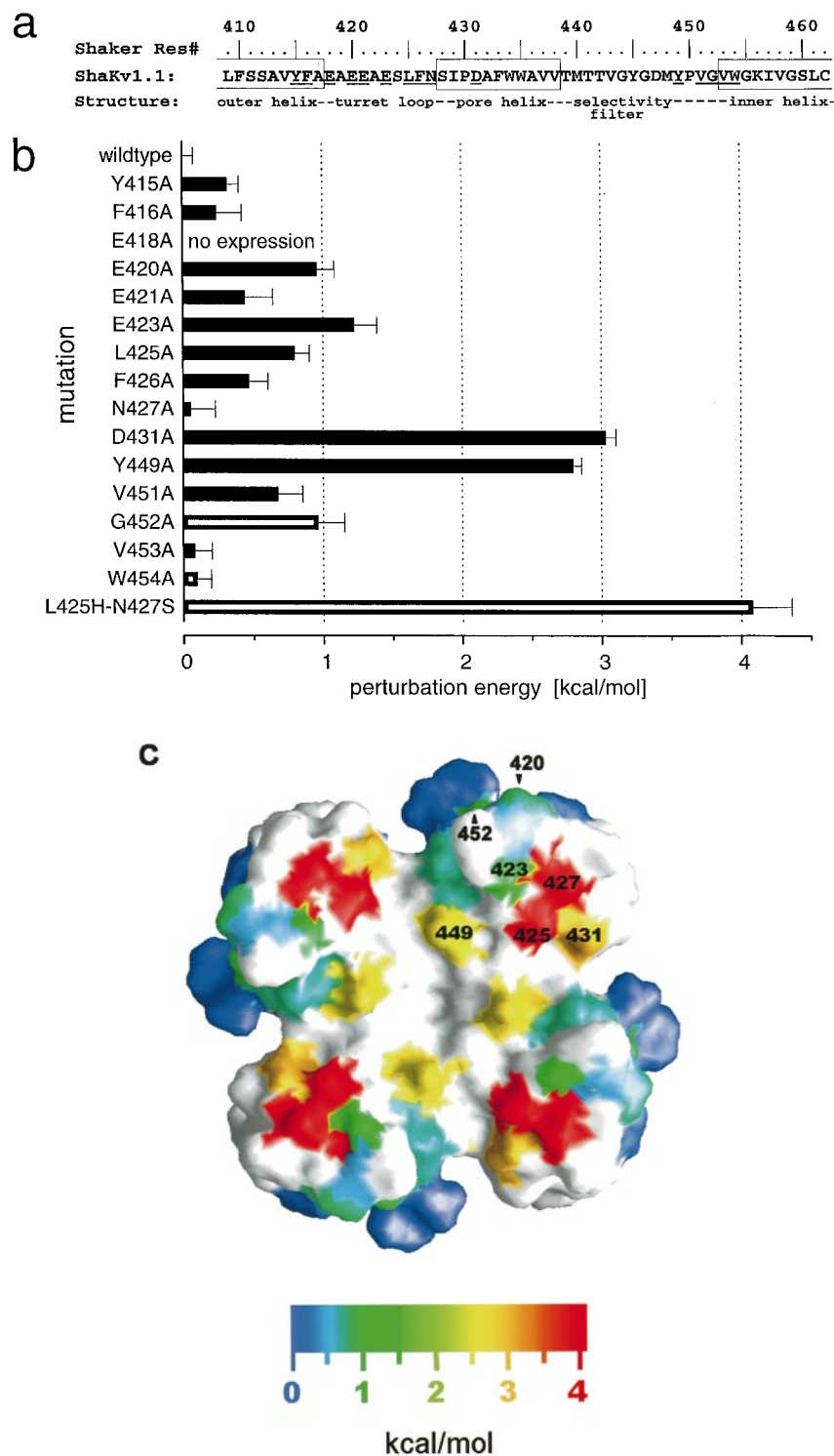


Figure 3. The dendrotoxin receptor surface of ShaKv1.1. (a) Pore region sequence of ShaKv1.1. Boxed regions are known to be helical in the structure of the KcsA K⁺ channel. Other regions are named after the structural elements identified in KcsA. Underlined residues indicate those individually substituted by alanine. Residues Leu425 and Asn427 were also jointly mutated to His and Ser residues, respectively. (b) Graph of the binding energy changes resulting from mutations relative to unmutated ShaKv1.1. Changes in binding energy were calculated as described in the legend to Figure 2(b). Empty bars denote increases, filled bars decreases in toxin affinity. The error bar represents the calculated error arising from propagation of the error in each K_d value (see Materials and Methods). No current could be measured through the expressed mutant channel Glu418Ala. (c) Surface representation of the pore region of KcsA viewed from the extracellular side looking down the axis of the pore (Doyle *et al.*, 1998; Acc. No.: 1BL8). The surface color represents the change in binding energy of δ -dendrotoxin (see color scale below) associated with a mutation at the equivalent residue position in ShaKv1.1. Non-mutated areas of the channel are white. Labeled residues are those with binding energy changes ≥ 0.9 kcal/mol. Residue positions 425 and 427 of ShaKv1.1 are colored according to the result obtained from their joint mutation Leu425His/Asn427-Ser.

resulted in binding free energy changes greater than 1 kcal mol⁻¹. Residues 420 and 452, which made significant but smaller contributions to toxin binding, are also labeled. The double mutation Leu425-His/Asn427Ser had the largest effect (>4 kcal mol⁻¹). This double mutation, as well as the Gly452Ala mutation, increased the affinity (open bars), while all other mutations decreased the affinity of toxin for the channel. Figure 3(c) shows that amino acid residues 423, 425 and 427 are located at

the apex of the turrets, while residue Asp431 lines the groove between. Residue Tyr449 lies immediately adjacent to the small central pore opening.

The consequences of an asymmetric ligand (in this case, dendrotoxin) binding to a 4-fold symmetric receptor (the K⁺ channel) are interesting, and have been considered in detail (MacKinnon, 1991b; Hidalgo & MacKinnon, 1995; Ranganathan *et al.*, 1996). Given a stoichiometry of one toxin per channel, when the toxin binds it can do so in one

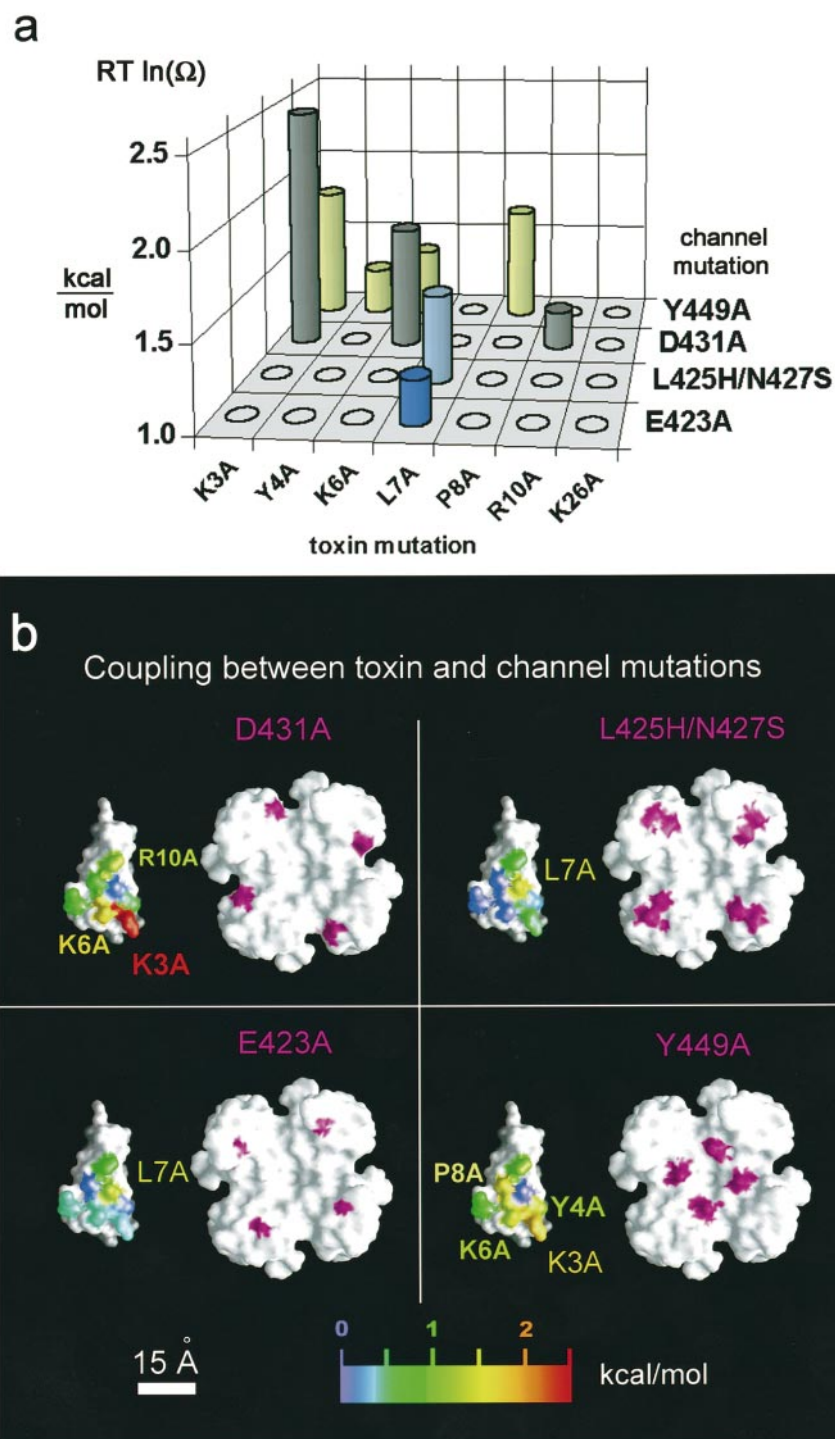


Figure 4. Non-additive (coupling) energies from double mutations. (a) Each indicated toxin mutant was tested against each of the shown channel mutants for those residues that are part of the functional interaction surfaces. The coupling energy (kcal mol^{-1}) for each toxin/channel pair was calculated according to equation (1). Table 1 lists the inhibition constants, K_d , used. Bars plot the coupling energy of those paired toxin/channel residue substitutions whose coupling energy exceeds 1 kcal mol^{-1} . See Table 1 for the complete listing of coupling energies of all toxin/channel residue pairs. (b) Views of the functional interaction surfaces of dendrotoxin and the K^+ channel. Each panel maps the coupling energies according to color and location for all functional interaction residues of dendrotoxin with the indicated channel mutant. Purple denotes the location of the channel mutation.

of four possible orientations. These orientations are energetically equivalent but statistically distinguishable. That is, the toxin can bind facing north, south, east or west. In any one orientation,

the toxin does not likely interact with all equivalent residues on the four subunits, because the toxin does not share the channel's molecular symmetry. Given the interaction surfaces defined on the toxin

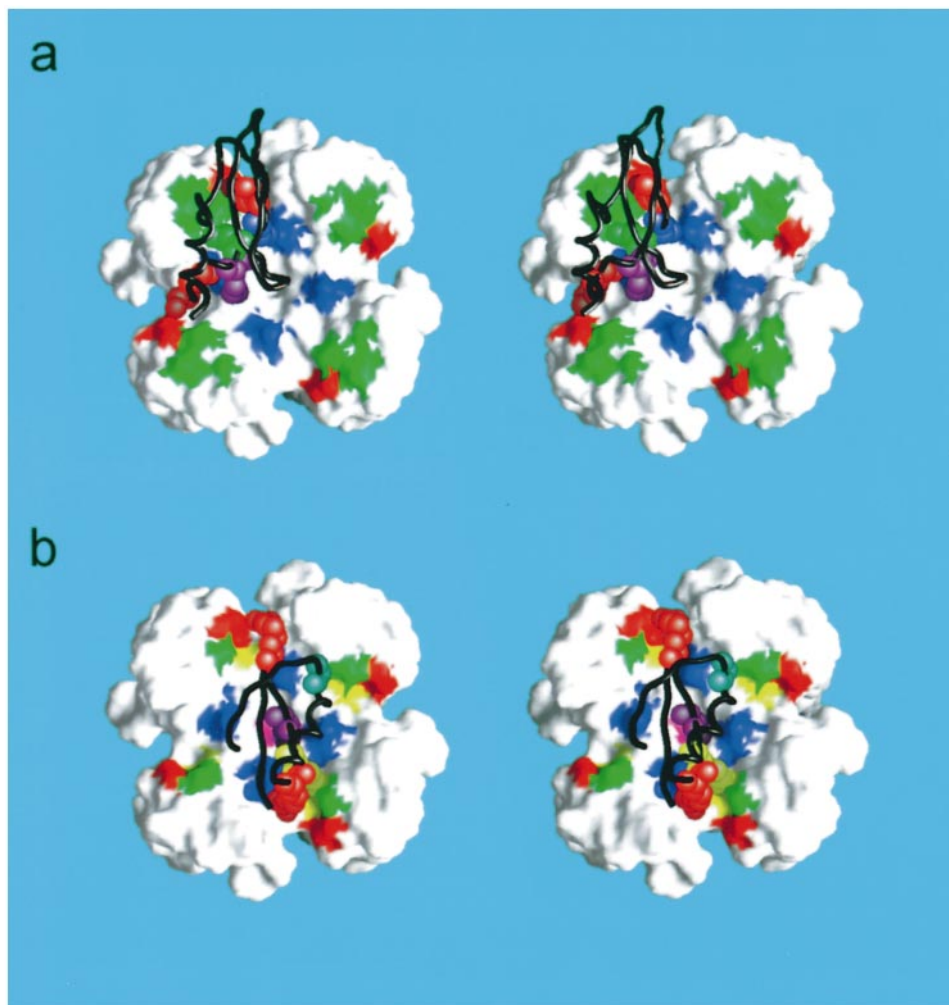


Figure 5. Hypothetical binding orientation for dendrotoxin. (a) Stereo diagram of δ -dendrotoxin relative to the Shaker K⁺ channel. The channel is shown in the same orientation as in Figure 3(c), looking directly down the pore from the extracellular side of the channel. The functional interaction residues of the channel have been mapped to the surface with the following color scheme: 423/425/427 (green), 431 (red), and 449 (blue). The toxin side-chains shown are from residues that strongly interact (through mutant cycles) with their color matched interaction partner(s) on the channel (Figure 4(a); Lys3 and Arg10, red; Leu7, green; Pro8, blue; Tyr4, omitted for clarity). Lys6 of δ -dendrotoxin, which interacts to roughly the same extent with both 431 (red) and 449 (blue), is purple. (b) Binding orientation of scorpion toxin on the K⁺ channel. This orientation is based on mutant cycle analysis of Agitoxin2 interaction with the Shaker channel (Ranganathan *et al.*, 1996; MacKinnon *et al.*, 1998). The channel residues are colored as in (a), except that positions 423 and 427 have been omitted. Additional Shaker residues that interact with Agitoxin2 are M448 (yellow) and Y445 (purple). The blue-green residue on Agitoxin2 interacts with both position 449 (blue) and 425 (green). The purple residue on Agitoxin2 is Lys27 which interacts with the external K⁺ binding site of the channel and thus acts as a “plug” in the pore (Park & Miller, 1992a,b; Ranganathan *et al.*, 1996). The orientation of the toxins relative to the channel was arrived at by visually minimizing the distances between the spacefilled models of the interacting toxin residue atoms (omitting hydrogen atoms) and the molecular surface of the coupled channel residues within the program GRASP (Nicholls *et al.*, 1991). The toxin backbones are shown as a black line.

and channel, with the concept of four mutually exclusive orientations in mind, we then tried to fit the two proteins together.

Interactions between mutations across the toxin-channel interface

To identify amino acid pairs that are near each other on the interface we looked for mutations whose effects are coupled according to thermodynamic mutant cycle analysis (Hidalgo & MacKinnon, 1995; Schreiber & Fersht, 1995). For

the seven amino acids forming the toxin interaction surface, paired with each of the four affinity-altering channel mutations, the K_d was determined for the four corners of a mutant cycle. The coupling coefficient, Ω , for the magnitude of interaction between any two perturbations is given by (Hidalgo & MacKinnon, 1995):

$$\Omega = \frac{K_d(wtX, wtY) \times K_d(mutX, mutY)}{K_d(wtX, mutY) \times K_d(mutX, wtX)} \quad (1)$$

where $K_d(X,Y)$ is the equilibrium dissociation con-

stant for toxin X and channel Y. An Ω deviating from unity indicates an interaction between the two mutations under study. In energetic terms, the coupling energy is given by the absolute value of $RT\ln(\Omega)$ and reflects the degree of non-additivity of the energetic effects of the single mutations. In the absence of large structural changes, coupled mutations should indicate close proximity on the protein-protein interface (Schreiber & Fersht, 1995).

Table 1 lists the K_d values as well as the coupling energies for the indicated toxin:channel mutant combinations. The mutant pairs giving rise to coupling energies greater than 1 kcal mol⁻¹ are plotted in the bar graph of Figure 4(a). The strongest coupling occurs between the channel mutation Asp431Ala and toxin mutation Lys3Ala. Asp431Ala is also coupled to mutation Lys6Ala and weakly but significantly to Arg10Ala. Lys3 and Lys6 are separated by one turn of a 3_{10} helix and therefore are quite near each other on δ -dendrotoxin. That mutation of the Lys residue at these two sites is coupled to mutation of the very same Asp on the channel is not surprising. Arg10, on the other hand, is almost 20 Å away from Lys3 on the dendrotoxin structure (Figure 2(c)). The Arg10Ala mutation is presumably coupled to mutation of an Asp431 residue on a separate subunit. Given the locations of the four Asp431 residues on the channel surface, a 20 Å distance is most consistent with the separation between two Asp431 residues on adjacent, rather than diagonal subunits (Figure 4(b)). Independent evidence supports this suggestion (below).

The double mutation Leu425His/Asn427Ser and single mutation Glu423Ala both couple uniquely to toxin mutation Leu7Ala (Figure 4(a)). These channel residues are located on the turret, while Leu7 is half way between Lys3 and Arg10 on the toxin interaction surface (Figure 4(b)). Since the turrets are located about half way between Asp431 residues on adjacent subunits, these assignments further suggest that dendrotoxin interacts predominantly with two adjacent subunits in the channel tetramer. The channel mutation Tyr449Ala couples to four separate mutations on the toxin (Figure 4(a)). These toxin mutations involve amino acids located near the base and to one side of Leu7 on the triangular interaction surface (Figure 4(b)).

Discussion

This study has defined a set of amino acids responsible for the binding of δ -dendrotoxin to a voltage-dependent K⁺ channel. The interaction surface on the toxin is a triangular patch of seven amino acids, four of which are basic. On the channel surface, the toxin interacts with amino acids that are located in the wide, shallow vestibule surrounding the extracellular pore entryway. Although dendrotoxins and scorpion toxins interact with many of the same amino acids on the K⁺ channel, mutant cycle analysis points to very

different docked complexes and mechanisms of action.

Figure 5(a) shows a hypothetical binding orientation for dendrotoxin that fulfills all of the mutant cycle derived constraints shown in Figure 4(b). In this model, the toxin is essentially draped over a turret with Leu7 in direct contact with turret amino acid residues. Lys3 and Arg10 reach into the grooves on either side of the turret where they are in close proximity to Asp431 residues from adjacent subunits. Lys6 is close enough to Lys3 to interact electrostatically with its Asp431 partner on the same subunit. The interaction of Tyr449 mutations with mutations of four toxin amino acid residues is also reasonably consistent with this orientation of the toxin with respect to the channel. We do not take this complex seriously in its detail, but rather, we propose that it will look something like that shown. In particular, the mutant cycle data provide very strong evidence that dendrotoxin binds off-center by interacting with a turret and two adjacent subunits. The major constraints pointing to this conclusion are the spatial assignments of Lys3 and Arg10, which are separated by about 20 Å, with Asp431 on the channel, and the assignment of Leu7 with turret amino acids in between Asp431 residues on adjacent subunits. Ultimately, this model will be tested with direct structural methods.

It is interesting to compare the mutant cycle derived constraints for agitoxin (a scorpion toxin) to those of dendrotoxin (Figure 5(a) and (b)). Agitoxin is smaller and fits into the groove between the turrets. It inhibits Shaker apparently by competing for part of the channel's "active site", the channel's outer K⁺ binding site, physically occluding the path of K⁺ ions (Park & Miller, 1992b; Ranganathan *et al.*, 1996). The channel amino acid residue Asp431 is very important in the interaction of both toxins, but mutations on agitoxin (involving Arg residues separated by 25 to 30 Å) are coupled to Asp431 on diagonal, not adjacent subunits (MacKinnon *et al.*, 1998).

The off-center location of dendrotoxin satisfies a subtle but important property of dendrotoxin-inhibited K⁺ channels: they are not always blocked completely. That is, with certain K⁺ channels, residual current flow may occur at very high toxin concentrations (Hall *et al.*, 1994; Owen *et al.*, 1997). At the single channel level, the residual current corresponds to a small but measurable current flow through the channel when the toxin is bound (Imredy *et al.*, 1998). Therefore, dendrotoxins reduce the flow of ions to a variable extent (depending on which K⁺ channel they are bound) but they do not prevent it altogether. In contrast, scorpion toxins seem to block the K⁺ current completely. An off-center binding site for dendrotoxin would leave a clear path for ion flow.

If dendrotoxins do not behave like molecular plugs, as do the scorpion toxins, then how do they inhibit K⁺ channels? It might be reasonable to suppose that the cationic toxin protein reduces K⁺

access to the pore by setting up a repulsive electrostatic potential (this kind of electrostatic mechanism has been proposed for μ conotoxin inhibition of sodium channels (French & Dudley, 1999)). However, in the case of dendrotoxin, our charge-altering mutations do not support such a mechanism (data not shown). We think it is more likely that the presence of dendrotoxin attached to the turret alters the dynamics of the pore and thus the throughput of ions. The pore region amino acids form a tightly packed unit consisting of the turret (which is very structured and resistant to proteases), pore helix, selectivity filter and an extended strand running radially away from the pore entryway (Doyle *et al.*, 1998). As ions move through the pore they undoubtedly distort its walls to some extent. If dendrotoxin binds and makes the structure more rigid, even to a small degree, then the flow of ions could be affected. Thus, we propose that dendrotoxins inhibit by altering the dynamical structure of the channel, not by capping its pore.

In the first Figure we showed a strange property of δ -dendrotoxin, that at extreme concentrations (one hundred times the K_d) it caused slow, irreversible inhibition of the K⁺ channel. This result is difficult to explain since at toxin concentrations of ten times K_d (90% inhibition), no irreversible inhibition is observed. This raises the possibility of a second, low affinity, but lethal site for dendrotoxin. However, toxin mutations that lower the affinity for reversible inhibition (the focus here) also proportionally lower the affinity for the irreversible inhibition, as if the sites are one and the same. Inspection of the proposed K⁺ channel-dendrotoxin complex raises an interesting but yet untested possibility. That is, that a second dendrotoxin could bind on the diagonally opposite turret. Due to steric hindrance, affinity for the second toxin would be much lower than for the first. But two toxins might induce an irreversible conformational change of the channel. This suggestion for irreversible inhibition is pure speculation but is directly testable.

Materials and Methods

Plasmids and mutagenesis

The *Drosophila melanogaster* Shaker H4 K⁺ channel was expressed using a clone (Kamb *et al.*, 1987) from which bases encoding amino acid residues 6-46 had been deleted, resulting in a non-inactivating K⁺ current (Hoshi *et al.*, 1990). All channel mutations were made in this background using a pore region cassette extending from *BsmI* (base 1153) to *SpeI* (base 1513).

A synthetic gene encoding δ -dendrotoxin (Imredy *et al.*, 1998) was inserted into the vector pCSP105 (Park *et al.*, 1991) using the *Sall/HindIII* cassette. δ -Dendrotoxin was expressed as a carboxy-terminal fusion to the capsid protein of T7 bacteriophage (gene 9 product) (Dunn & Studier, 1983). δ -Dendrotoxin and channel mutations were generated using a sequential PCR protocol. All

mutations were verified by sequencing the entire cassette after its reinsertion into the plasmid.

Electrophysiological assay of δ -dendrotoxin

The electrophysiological recording of K⁺ currents was performed according to previously published methods (Imredy *et al.*, 1998). *In vitro* transcribed mutant Shaker channel mRNA was injected into defolliculated oocytes isolated from *Xenopus laevis* frogs (Oocyte One, Michigan; NASCO, Wisconsin) one day after surgical harvesting and collagenase treatment (Worthington, Type II, 0.5 mg/ml for one hour) of fresh oocytes. Expressed K⁺ currents were recorded with a two-electrode voltage-clamp recording amplifier (Warner Instruments OC-725A) within four days of injection. For recording, the oocytes were placed in a 130 μ l bath and continuously perfused with a frog Ringer solution containing 96 mM NaCl, 2 mM KCl, 0.3 mM CaCl₂, 1 mM MgCl₂, 0.05 mg/ml bovine serum albumin (SIGMA), and 5 mM Hepes at pH 7.6 (NaOH). Just prior to its application to the recording chamber, δ -dendrotoxin was added to the perfusate from a stock kept at 4°C (or on ice) in 100 mM Hepes at pH 7.6 (NaOH). To determine the fraction of total dendrotoxin-sensitive current, a high concentration (100-1000 times K_d) was added to the recording chamber. For concentrations ≥ 10 mM the flow was stopped and the toxin was added directly to the flow chamber. Inhibition curves always refer to this dendrotoxin-sensitive current. For the currents shown in Figure 1, a solution containing 100 mM TEACl, 2 mM KCl, 0.3 mM CaCl₂, 1 mM MgCl₂, 0.05 mg/ml bovine serum albumin, and 5 mM Hepes at pH 7.6 (NaOH) was perfused, and the remaining current was used to subtract capacitive and TEA insensitive leak current.

In order to evoke K⁺ current through Shaker channels, depolarizing potential steps of 300 ms duration and 80 mV magnitude were applied to oocytes from a resting potential of -80 mV. The elicited current was recorded digitally and stored on a computer. The average current value during the last 15 ms of a given current response (Figure 1(c)) was used as a measure of the K⁺ current during that pulse (Figure 1(b)). All electrophysiological recordings were performed at room temperature. Fits of the Langmuir isotherm to dendrotoxin K⁺ current inhibition plots (Figure 1(d)) were made using Origin software (Microcal, Massachusetts). The error in the binding energy and coupling energy values (Figures 2, 3 and 4) were calculated from the experimental error of the measured K_d values (reported as the standard error of the mean, or SEM) using the geometric sum of the partial errors. For $f(x,y)$, a function of two inhibition constants, x and y , the resulting error in the function, Δf , was approximated by:

$$\Delta f = \sqrt{\left(\frac{\partial f}{\partial x} \Delta x\right)^2 + \left(\frac{\partial f}{\partial y} \Delta y\right)^2}$$

where Δx and Δy are the measured errors in the inhibition constants (SEM).

Expression and purification of δ -dendrotoxin

The expression and purification procedure for δ -dendrotoxin followed previously established methods (Imredy *et al.*, 1998). δ -Dendrotoxin was expressed in the BL21-DE3 strain of *E. coli* as a carboxy-terminal fusion to the T7 bacteriophage capsid protein (gene 9 product) fol-

lowed by an engineered Factor Xa cleavage recognition site. The fusion protein was isolated using anion exchange chromatography on a DE52 (Whatman) packed column. In the case of all but two of the dendrotoxin mutations the dendrotoxin, cleaved from its fusion partner by trypsin, could be isolated as a functional protein with the correct mass spectrogram. The dendrotoxin mutants Arg44Ala and Asn41Ala, however, had to be cleaved with Factor Xa from the fusion protein in order to be isolated. Following its cleavage, the toxin was isolated using cation exchange chromatography (Mono S, Pharmacia Biotech). The eluted dendrotoxin solution was desalted and purified using HPLC reverse phase chromatography (VYDAC C8, Phenomenex). The calculated extinction coefficient of $17,883 \text{ M}^{-1} \text{ cm}^{-1}$ (Imredy *et al.*, 1998) was used to estimate the concentration of wild-type and mutated dendrotoxins except for mutations involving alanine residue substitutions for Tyr and Trp residues. For estimation of these mutant toxin concentrations, the extinction coefficients were adjusted (Gill & von Hippel, 1989).

Acknowledgments

We thank Natalia Rodionova for mass spectrometric validation of purified dendrotoxins, Benoit Roux for his suggestions and advice, and Wendell Chin for help with the preparation of the manuscript. The members of the MacKinnon laboratory provided a variety of invaluable suggestions throughout the course of this work, especially João Morais Cabral and Jacqueline Gulbis. This work was supported by NIH grant GM43949. R.M. is an Investigator in the Howard Hughes Medical Institute.

References

- Anderson, A. J. (1985). The effects of protease inhibitor homologues from mamba snake venoms on autonomic neurotransmission. *Toxicon*, **23**, 947-954.
- Bagust, J., Zhang, L. & Owen, D. (1997). Toxin I, but not 4-aminopyridine, blocks the late inhibitory component of the dorsal root reflex in an isolated preparation of rat spinal cord. *Brain Res.* **773**, 181-189.
- Becker, S., Prusak-Sochaczewski, E., Zamponi, G., Beck-Sickinger, A. G., Gordon, R. D. & French, R. J. (1992). Action of derivatives of μ -conotoxin GIIIA on sodium channels. Single amino acid substitutions in the toxin separately affect association and dissociation rates. *Biochemistry*, **31**, 8229-8238.
- Beeser, S. A., Goldenberg, D. P. & Oas, T. G. (1997). Enhanced protein flexibility caused by a destabilizing amino acid replacement in BPTI. *J. Mol. Biol.* **269**, 154-164.
- Benishin, C. G., Sorensen, R. G., Brown, W. E., Krueger, B. K. & Blaustein, M. P. (1988). Four polypeptide components of green mamba venom selectively block certain potassium channels in rat brain synaptosomes. *Mol. Pharmacol.* **34**, 152-159.
- Berndt, K. D., Guntert, P. & Wuthrich, K. (1993). Nuclear magnetic resonance solution structure of dendrotoxin K from the venom of *Dendroaspis polylepis polylepis*. *J. Mol. Biol.* **234**, 735-750.
- Black, A. R., Breeze, A. L., Othman, I. B. & Dolly, J. O. (1986). Involvement of neuronal acceptors for dendrotoxin in its convulsive action in rat brain. *Biochem. J.* **237**, 397-404.
- Clackson, T. & Wells, J. A. (1995). A hot spot of binding energy in a hormone-receptor interface. *Science*, **267**, 383-386.
- Collier, B., Padjen, A. L., Quik, M. & Smith, P. A. (1981). Convulsant and possible anticholinergic actions of dendrotoxin in the amphibian spinal cord. *Br. J. Pharmacol.* **73**, 525-533.
- Dolly, J. O. & Parcej, D. N. (1996). Molecular properties of voltage-gated K⁺ channels. *J. Bioenerg. Biomembr.* **28**, 231-253.
- Doyle, D. A., Morais, C. J., Pfuetzner, R. A., Kuo, A., Gulbis, J. M., Cohen, S. L., Chait, B. T. & MacKinnon, R. (1998). The structure of the potassium channel: molecular basis of K⁺ conduction and selectivity. *Science*, **280**, 69-77.
- Dufton, M. J. (1985). Proteinase inhibitors and dendrotoxins. Sequence classification, structural prediction and structure/activity. *Eur. J. Biochem.* **153**, 647-654.
- Dunn, J. J. & Studier, F. W. (1983). Complete nucleotide sequence of bacteriophage T7 DNA and the locations of T7 genetic elements. *J. Mol. Biol.* **166**, 477-535.
- French, R. J. & Dudley, S. C., Jr (1999). Pore-blocking toxins as probes of voltage-dependent channels. *Methods Enzymol.* **294**, 575-605.
- Gasparini, S., Danse, J. M., Lecoq, A., Pinkasfeld, S., Zinn-Justin, S., Young, L. C., de Medeiros, C. C., Rowan, E. G., Harvey, A. L. & Menez, A. (1998). Delineation of the functional site of alpha-dendrotoxin. The functional topographies of dendrotoxins are different but share a conserved core with those of other Kv1 potassium channel-blocking toxins. *J. Biol. Chem.* **273**, 25393-25403.
- Gill, S. C. & von Hippel, P. H. (1989). Calculation of protein extinction coefficients from amino acid sequence data. *Anal. Biochem.* **182**, 319-326.
- Hall, A., Stow, J., Sorensen, R., Dolly, J. O. & Owen, D. (1994). Blockade by dendrotoxin homologues of voltage-dependent K⁺ currents in cultured sensory neurones from neonatal rats. *Br. J. Pharmacol.* **113**, 959-967.
- Halliwel, J. V., Othman, I. B., Pelchen-Matthews, A. & Dolly, J. O. (1986). Central action of dendrotoxin: selective reduction of a transient K conductance in hippocampus and binding to localized acceptors. *Proc. Natl Acad. Sci. USA*, **83**, 493-497.
- Harvey, A. L. (1997). Recent studies on dendrotoxins and potassium ion channels. *Gen. Pharmacol.* **28**, 7-12.
- Harvey, A. L. & Anderson, A. J. (1985). Dendrotoxins: snake toxins that block potassium channels and facilitate neurotransmitter release. *Pharmacol. Ther.* **31**, 33-55.
- Harvey, A. L. & Gage, P. W. (1981). Increase of evoked release of acetylcholine at the neuromuscular junction by a fraction from the venom of the eastern green mamba snake (*Dendroaspis angusticeps*). *Toxicon*, **19**, 373-381.
- Hidalgo, P. & MacKinnon, R. (1995). Revealing the architecture of a K⁺ channel pore through mutant cycles with a peptide inhibitor. *Science*, **268**, 307-310.
- Hollecker, M. & Creighton, T. E. (1983). Evolutionary conservation and variation of protein folding pathways. Two protease inhibitor homologues from black mamba venom. *J. Mol. Biol.* **168**, 409-437.

- Hoshi, T., Zagotta, W. N. & Aldrich, R. W. (1990). Biophysical and molecular mechanisms of Shaker potassium channel inactivation. *Science*, **250**, 533-538.
- Hurst, R. S., Busch, A. E., Kavanaugh, M. P., Osborne, P. B., North, R. A. & Adelman, J. P. (1991). Identification of amino acid residues involved in dendrotoxin block of rat voltage-dependent potassium channels. *Mol. Pharmacol.* **40**, 572-576.
- Imredy, J. P., Chen, C. & MacKinnon, R. (1998). A snake toxin inhibitor of inward rectifier potassium channel ROMK1. *Biochemistry*, **37**, 14867-14874.
- Joubert, F. J. & Taljaard, N. (1980). Snake venoms. The amino acid sequences of two proteinase inhibitor homologues from *Dendroaspis angusticeps* venom. *Hoppe Seylers Z. Physiol. Chem.* **361**, 661-674.
- Kamb, A., Iverson, L. E. & Tanouye, M. A. (1987). Molecular characterization of *Shaker*, a *Drosophila* gene that encodes a potassium channel. *Cell*, **50**, 405-413.
- Kraulis, P. J. (1991). MOLSCRIPT: a program to produce both detailed and schematic plots of protein structures. *J. Appl. Crystallog.* **24**, 946-950.
- MacKinnon, R. (1991a). Using mutagenesis to study potassium channel mechanisms. *J. Bioenerg. Biomembr.* **23**, 647-663.
- MacKinnon, R. (1991b). Determination of the subunit stoichiometry of a voltage-activated potassium channel. *Nature*, **350**, 232-235.
- MacKinnon, R., Cohen, S. L., Kuo, A., Lee, A. & Chait, B. T. (1998). Structural conservation in prokaryotic and eukaryotic potassium channels. *Science*, **280**, 106-109.
- Miller, C. (1995). The charybdotoxin family of K⁺ channel-blocking peptides. *Neuron*, **15**, 5-10.
- Nicholls, A., Sharp, K. & Honig, B. (1991). Protein folding and association: insights from the interfacial and thermodynamic properties of hydrocarbons. *Proteins: Struct. Funct. Genet.* **11**, 281-296.
- Owen, D. G., Hall, A., Stephens, G., Stow, J. & Robertson, B. (1997). The relative potencies of dendrotoxins as blockers of the cloned voltage-gated K⁺ channel, mKv1.1 (MK-1), when stably expressed in Chinese hamster ovary cells. *Br. J. Pharmacol.* **120**, 1029-1034.
- Parcej, D. N. & Dolly, J. O. (1989). Dendrotoxin acceptor from bovine synaptic plasma membranes. Binding properties, purification and subunit composition of a putative constituent of certain voltage-activated K⁺ channels. *Biochem. J.* **257**, 899-903.
- Park, C. S. & Miller, C. (1992a). Mapping function to structure in a channel-blocking peptide: electrostatic mutants of charybdotoxin. *Biochemistry*, **31**, 7749-7755.
- Park, C. S. & Miller, C. (1992b). Interaction of charybdotoxin with permeant ions inside the pore of a K⁺ channel. *Neuron*, **9**, 307-313.
- Park, C. S., Hausdorff, S. F. & Miller, C. (1991). Design, synthesis, and functional expression of a gene for charybdotoxin, a peptide blocker of K⁺ channels. *Proc. Natl Acad. Sci. USA*, **88**, 2046-2050.
- Pongs, O. (1990). Structural basis of potassium channel diversity in the nervous system. *J. Basic Clin. Physiol. Pharmacol.* **1**, 31-39.
- Pongs, O. (1993). Receptor sites for open channel blockers of *Shaker* voltage-gated potassium channels-molecular approaches. *J. Recept. Res.* **13**, 503-512.
- Ranganathan, R., Lewis, J. H. & MacKinnon, R. (1996). Spatial localization of the K⁺ channel selectivity filter by mutant cycle-based structure analysis. *Neuron*, **16**, 131-139.
- Rehm, H. & Lazdunski, M. (1988). Purification and subunit structure of a putative K⁺-channel protein identified by its binding properties for dendrotoxin I. *Proc. Natl Acad. Sci. USA*, **85**, 4919-4923.
- Schreiber, G. & Fersht, A. R. (1995). Energetics of protein-protein interactions: analysis of the barnase-barstar interface by single mutations and double mutant cycles. *J. Mol. Biol.* **248**, 478-486.
- Sigworth, F. J. (1994). Voltage gating of ion channels. *Quart. Rev. Biophys.* **27**, 1-40.
- Silveira, R., Barbeito, L. & Dajas, F. (1988a). Behavioral and neurochemical effects of intraperitoneally injected dendrotoxin. *Toxicon*, **26**, 287-292.
- Silveira, R., Siciliano, J., Abo, V., Viera, L. & Dajas, F. (1988b). Intraatrial dendrotoxin injection: behavioral and neurochemical effects. *Toxicon*, **26**, 1009-1015.
- Smith, L. A., Reid, P. F., Wang, F. C., Parcej, D. N., Schmidt, J. J., Olson, M. A. & Dolly, J. O. (1997). Site-directed mutagenesis of dendrotoxin K reveals amino acids critical for its interaction with neuronal K⁺ channels. *Biochemistry*, **36**, 7690-7696.
- Stocker, M., Pongs, O., Hoth, M., Heinemann, S. H., Stuhmer, W., Schroter, K. H. & Ruppersberg, J. P. (1991). Swapping of functional domains in voltage-gated K⁺ channels. *Proc. Roy. Soc. Lond. Biol. Sci.* **245**, 101-107.
- Tytgat, J., Debont, T., Carmeliet, E. & Daenens, P. (1995). The alpha-dendrotoxin footprint on a mammalian potassium channel. *J. Biol. Chem.* **270**, 24776-24781.
- Velluti, J. C., Caputi, A. & Macadar, O. (1987). Limbic epilepsy induced in the rat by dendrotoxin, a polypeptide isolated from the green mamba (*Dendroaspis angusticeps*) venom. *Toxicon*, **25**, 649-657.
- Wang, F. C., Bell, N., Reid, P., Smith, L. A., McIntosh, P., Robertson, B. & Dolly, J. O. (1999). Identification of residues in dendrotoxin K responsible for its discrimination between neuronal K⁺ channels containing Kv1.1 and 1.2 alpha subunits. *Eur. J. Biochem.* **263**, 222-229.
- Yellen, G. (1998). The moving parts of voltage-gated ion channels. *Quart. Rev. Biophys.* **31**, 239-295.

Edited by G. von Heijne

(Received 6 October 1999; received in revised form 12 January 1999; accepted 13 January 1999)